ANNALS of Faculty Engineering Hunedoara
– International Journal of Engineering
Tome XIV [2016] – Fascicule 4 [November]
ISSN: 1584-2665 [print; online]
ISSN: 1584-2673 [CD-Rom; online]
a free-access multidisciplinary publication
of the Faculty of Engineering Hunedoara

[1.]Lin HANHUI, [2.]Cai KEN, [3.]Chen HUAZHOU,
[4.]Zeng ZHAOFENG

# OPTIMIZATION DESIGN OF FRUIT PINKING END-EFFECTOR BASED ON ITS GRASPING MODEL

[1.] Center for Educational Technology, Guangdong University of Finance & Economics, Guangzhou, CHINA
[2.] School of Information Science and Technology, Zhongkai University of Agriculture and Engineering, Guangzhou, CHINA
[3.] College of Science, Guilin University of Technology, Guilin, CHINA
[4.] Department of Mathematics and Computer Science, California State University, East Bay, U.S.A

**ABSTRACT**: The development of intelligent fruit harvesting robots is important in improving agricultural production. In this paper, we initiated the R&D of a mechanical end-effector for fruit harvesting on the basis of the intelligence of agricultural robots. First, we provided a detailed description of the hardware components and software control of the mechanical end-effector, analyzed the mechanism of servo controlling and established a mathematical modeling of the mechanical end-effector junctions by analyzing the harvesting movement. Thereafter, the coordinates of the target fruits are disassembled and analyzed in the context of the mathematical model for precise locating and harvesting. Finally, a trail experiment of harvesting kiwifruit was conducted. The outcome implies that each module in the harvesting robot system functions well. The proposed mathematical modeling method and servo control can provide accurate harvesting movements to the mechanical end-effector.
**Keywords**: picking, end-effector, motion optimization, models

## 1. INTRODUCTION

Great efforts have been made in the past decades in the use of robots for selective harvesting, which is the most time-consuming process in agricultural operations. In natural environments, the growth of fruits depends on soil, season, and weather, which varies enormously and hinders precise locating and harvesting. Therefore, the research and development of high-end robots with accuracy and efficiency has become increasingly significant in agricultural harvesting [2,8,10,11]. Such a study has been performed for more than 40 years in many countries [16,21,18,6]. Japan, the United States, and some developed European countries have been working relentlessly on the R&D of harvesting robots. In Japan, eggplant-harvesting robots spend 64.1 s in picking one eggplant and have success rates of 62.5% [7]. Grape-harvesting robots are not only capable of harvesting but also of spraying, bagging, and clipping [1]. Kiwifruit-harvesting robots have harvesting speeds of 74.6 s for each fruit and suction attachment success rates of 95.3% [3]. Wageningen University designed cucumber-harvesting robots that utilize near-infrared visual system to identify cucumbers with success rates of approximately 70% [15]. Mushroom-harvesting robots designed in the United Kingdom can harvest one mushroom in 1.5 s with a success rate of 75% [4]. Melon-harvesting robots designed in Israel and the United States can achieve a success rate of over 85% during identification and harvesting [5]. The apple-harvesting robots developed by Kyungpook National University in South Korea can identify cucumbers from the tree crown with a success rate of 85% and harvesting speed of 5 s for each cucumber [17]. The mushroom-harvesting robots by Silsoe Research Institute in the United Kingdom can harvest at the speed of 6.7 s for each mushroom with a success rate of 75% [13]. In China, the study of harvesting robots has made significant progress in recent years. China

Agricultural University has developed cucumber-harvesting robots and vegetable-grafting robots [20, 9], Nanjing Agricultural University has furthered the visual navigation system to enable automatic operations [22], and Zhejiang University has designed and optimized the visual positioning and harvesting components of robots [19]. All of these studies have accelerated the development of agricultural informatization and automation in China. In the present paper, the position coordinates of fruits were obtained from a binocular system. The necessary movement at each end-effector junction was controlled according to the 3D coordinate analytic algorithm. The revolving angle of each servo was manipulated to stretch the mechanical arm to the target fruit and for harvesting.

## 2. MATERIALS AND METHODS

### The Harvesting End-effector

The system uses an end-effector (Figure 1) that is made of aluminum alloy brackets and servos. The entire end-effector is equipped with two MG995 servos and three MG996R servos. The picking tool has a highly mimicking design. In harvesting, only No.3, No.4, No.5, No.6, and No.7 servos are involved, whereas the No.2 servo is a back-up that is temporarily immovable and is vertically upward. The No.3 servo controls the base rotation, thereby controlling the movement direction of the picking robot. The No.4 and No.5 servos control the main body of the arm, which is equivalent to the hand control of humans controlling lifting and other actions. The No.6 servo, the equivalent of a human's wrist, controls the vertical movement when picking fruits. The No.7 servo controls the opening or closing of metal pincers, similar to a human's fingers. The respective location of each servo in the harvesting end-effector is shown in Figure 1(a).

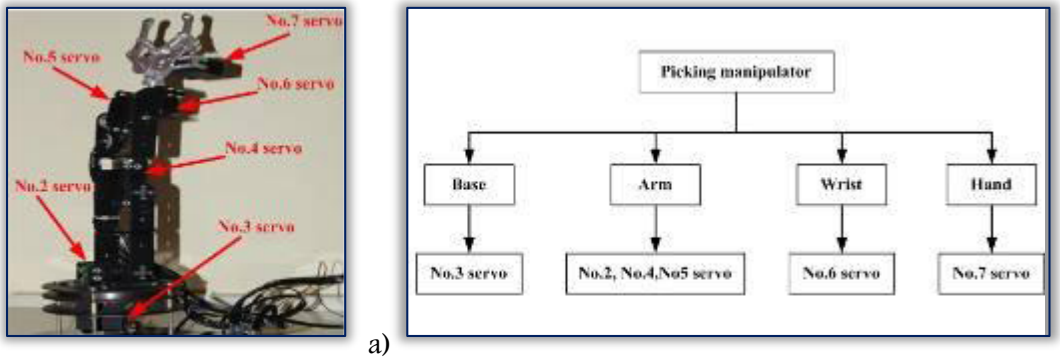


a) b)

Figure1- Picking robot chart. (a) The specific location of each servo. (b) Picking end-effector joint control.

### Control of Harvesting End-effector and Motion Analysis

The servo control uses a PWM signal with a unique time width between high and low levels [12]. Given that the servo system uses a digital servo type, it has a low requirement for PWM signal. Furthermore, the servo system does not need to receive real-time instruction and can be auto-locked and positioned. These characteristics have outperformed the ordinary stepper motor [14]. The timing diagram of the PWM signal is shown in Figure 2.

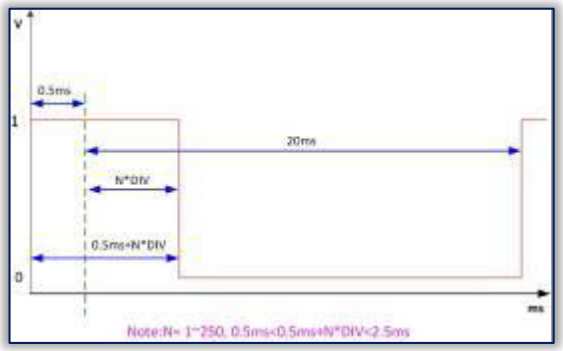


Figure 2 - PWM timing diagram at one cycle

The servo system used for the harvesting end-effector has no requirement for low-level time, thus indicating that the use of a low time of 0.5 ms is allowable and that a cycle of the PWM waveform can be 1 ms standard square wave. The system controller uses an 8-bit micro-controller and 256 data resolution, which will be divided into 250 parts after the servo limit parameter experiment. Thereafter, when the width between 0.5 ms to 2.5 ms is 2000 μs, the width will be divided into 250 parts, thus resulting to 8 μs. The PWM control precision can be used to control the revolving and positioning of the servo at an increasing basis. Given that the servo can revolve at 185°, the servo's control precision is 0.74°. By controlling the servo's revolving angle according to PWM wave high-level duration, we obtained the data shown in Table 1 to Table 5. The 0° angle in the Tables represents the critical point in the positive and negative directions of the space coordinates. Table 1 to Table 5 shows that the revolving angle of servo has a linear relation with PWM wave high-level duration.

Table 1. Relation between No.3 servo's revolving angle and PWM wave high-level duration

| Angle (°) | −72 | −45 | −30 | 0 | 60 |
|---|---|---|---|---|---|
| High-level voltage (μs) | 2000 | 1775 | 1588 | 1380 | 1000 |

Table 2. Relation between No.4 servo's revolving angle and PWM wave high-level duration

| Angle (°) | −50 | −35 | 0 | 45 | 90 |
|---|---|---|---|---|---|
| High-level voltage (μs) | 2100 | 2000 | 1760 | 1380 | 1000 |

Table 3. Relation between No.5 servo's revolving angle and PWM wave high-level duration

| Angle (°) | −45 | 0 | 90 | 143 |
|---|---|---|---|---|
| High-level voltage (μs) | 500 | 800 | 1470 | 2100 |

Table 4. Relation between No.6 servo's revolving angle and PWM wave high-level duration

| Angle (°) | −14 | 0 | 90 | 173 |
|---|---|---|---|---|
| High-level voltage (us) | 500 | 620 | 1380 | 2000 |

Table 5. Relation between No.7 servo's revolving angle and PWM wave high-level duration

| Angle (°) | 0 | 24 | 37 | 49 |
|---|---|---|---|---|
| High-level voltage (μs) | 2100 | 1850 | 1720 | 1600 |

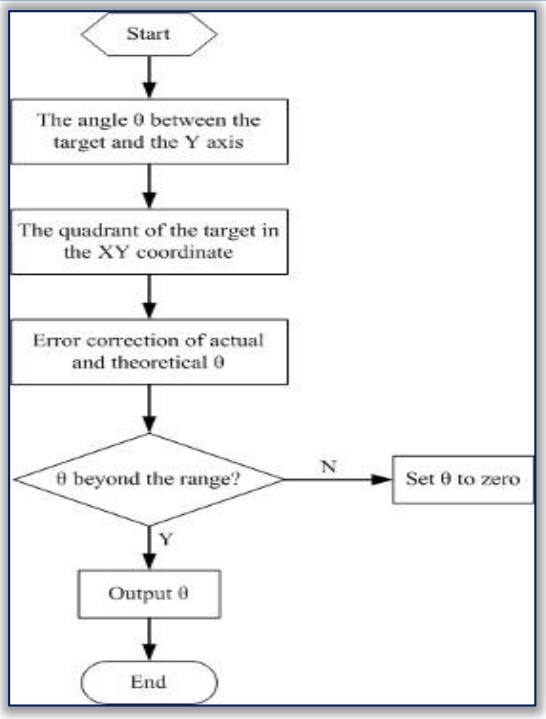


Figure 3 ~ Flow chart of No.3 servo's revolving angle

## 3. CLASSIFICATION AND COORDINATE COMPOSITION OF HARVESTING MOVEMENT

In harvesting, only the No.3, No.4, No.5, No.6, and No.7 servos are involved, whereas the No.2 servo is a back-up that is temporarily immovable and is vertically upward. The No.6 and No.7 servos control the picking and stabilization of the kiwifruit, respectively. Thus, the No.6 and No.7 servos do not involve the end-effector's accurate movements to the target kiwifruit. The No.3 servo controls the base rotation, thereby controlling the revolving angle according to the X and Y space coordinates of the target kiwifruit. The flow chart of the programming is shown in Figure 3.

Only determining the rotational angle of the No.3 servo is insufficient to move the end-effector's clamp to the target kiwifruit. This movement needs the analysis of the revolving angles of the No.4 and No.5 servos. The force manipulators that are controlled by the No.4 and No.5 servos are named as ahead arm and rear arm, respectively. As shown in Figure 4, the target kiwifruit is set as point A, the No.4 servo as one point, and the No.5 as another point. A triangle is formed by connecting the three points.

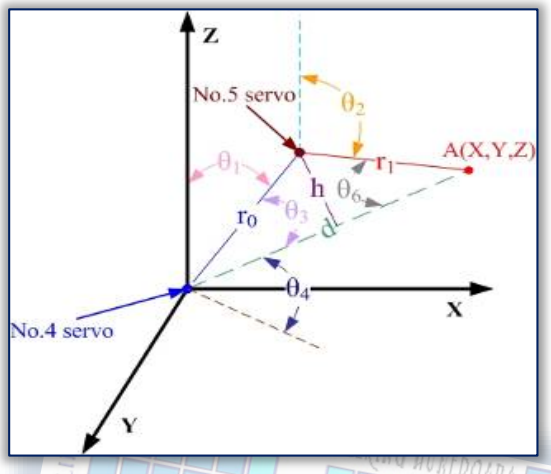


Figure 4 ~ Mathematical modeling of revolving angles of No.4 and No.5 servos

In Figure 4, $\theta_1$ and $\theta_2$ are the revolving angles of the No.4 and No.5 servos, respectively; $r_0$ and $r_1$ represent the distances from the No.4 to No.5 servos and No.5 to No.6 servos, respectively. The distance d from point A to original point "O" in Figure 4 can be obtained by using the XYZ coordinates transmitted by the binocular system.

$$d = \sqrt{X^2 + Y^2 + Z^2} \quad (1)$$

The triangle's heighth can be calculated by Heron's formula:

$$h = \frac{2\sqrt{p(p-r_0)(p-r_1)(p-d)}}{d} \quad (2)$$

where p is the half perimeter defined by the following:

$$p = \frac{1}{2}(r_0 + r_1 + d) \quad (3)$$

By using $r_0$, $r_1$, and height h with anti-trigonometric function, angles $\theta_3$ and $\theta_6$ in this triangle can be acquired as follows:

$$\theta_3 = \arcsin(\frac{h}{r_0}) \qquad \theta_6 = \arcsin(\frac{h}{r_1}) \tag{4}\text{-}(5)$$

By using the Z coordinates of the target kiwifruit, angle $\theta_4$ of line segment OA and the horizontal plane can be calculated as follows:

$$\theta_4 = \arcsin(\frac{|Z|}{d}) \tag{6}$$

Finally, according to the law of therightangle, $\theta_1$ and $\theta_2$ are given by the following:

$$\theta_1 = 90^\circ - \theta_3 - \theta_4 \qquad \theta_2 = 90^\circ - \theta_4 + \theta_6 \tag{7}\text{-}(8)$$

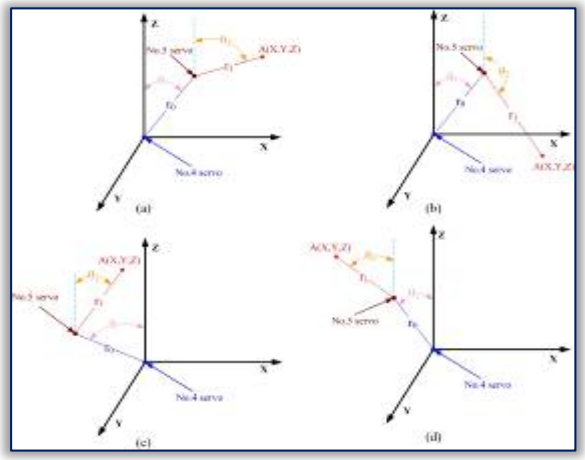

Figure 5 - Flow chart of receiving the coordinates by the end-effector's controller

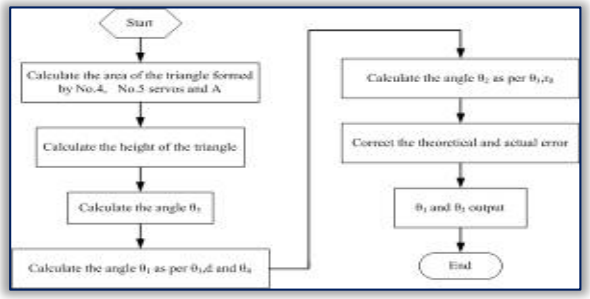


Figure 6 - Flow chart of picking feedback

The calculation algorithm of the steering revolving angle of the No.4 and No.5 servos is limited to the right ahead and above direction. Thus, $\theta_1$ has a positive degree value and $\theta_2$ is less than 90°. However, in actual conditions, the harvesting system is operated on the ground where complicated directions are involved such as ahead above, rear above, ahead below, and rear below. According to various experiments, the picking robot only needs four postures to achieve 360° of harvesting operation. The four postures are quite similar to a human's hand–wrist movements in all directions. As shown in Figure 5, the end-effector has four corresponding picking postures. The picking postures are distinguished on the basis of the revolving angle of over ±90°. Figure 6 shows the programming flow chart of how an end-effector controls the revolving angle of the No.4 and No.5 servos according to the space coordinates of the target fruit.

## 4. COMMUNICATION BETWEEN THE END-EFFECTOR AND PC

The control system communicates with a PC through serial ports. When a PC detects a kiwifruit, it calculates the space coordinates of the target fruit. The PC will then transmit 9600 b/s baud rate of data to the control system of the robot end-effector. Given that the communication between the PC and the end-effector's controller can only transmit one 8 bit binary data, a special algorithm needs to be applied to the data conversion to protect the data validity within the scope of 8 bit binary data and the data must be stored in the end-effector's controller.

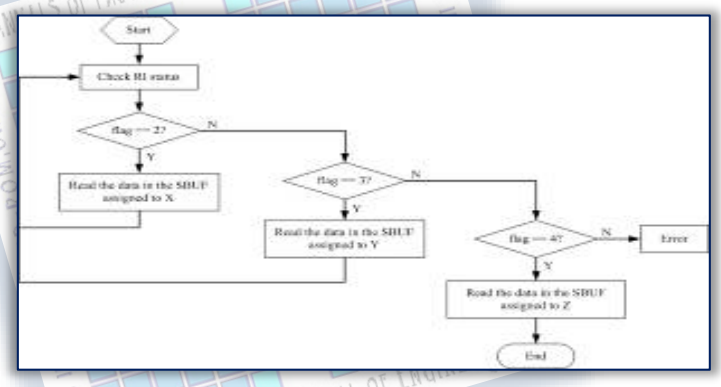


Figure 7- Flow chart of receiving the coordinates by the end-effector's controller

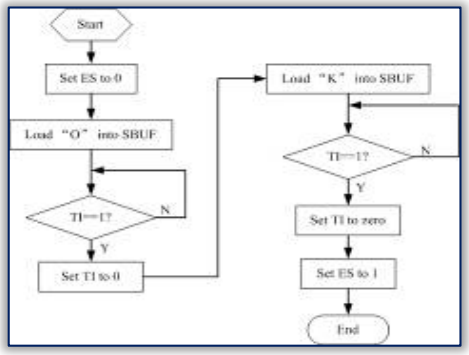


Figure 8 - Flow chart of picking feedback

The program of the specific data receiving the unit of the harvesting end-effector is shown in Figure 7. When the communication of serial ports is interrupted, RI is the zero setting and the flag

denotes the flag bit of the data transmitted. The data transmitted from the PC is the X-axis coordinate, which is followed by Y and Z coordinates.

When the picking end-effector completes a set of assigned actions according to the given coordinates and finally picked up the target kiwifruit, the end-effector will respond with an "OK" feedback to the PC as a signal for the picking order of the next target. The "OK" feedback procedure code is shown in Figure 8. First, ES is set to zero and "O" is placed in SBUF for data storage. Thereafter, TI is tested if it has a value of one to determine if the PC received the data. The same procedure is adopted to "K," and ES is set to one.

## 5. RESULTS

This paper selects clusters of fruits to be picked. The process is shown in Figure 9.

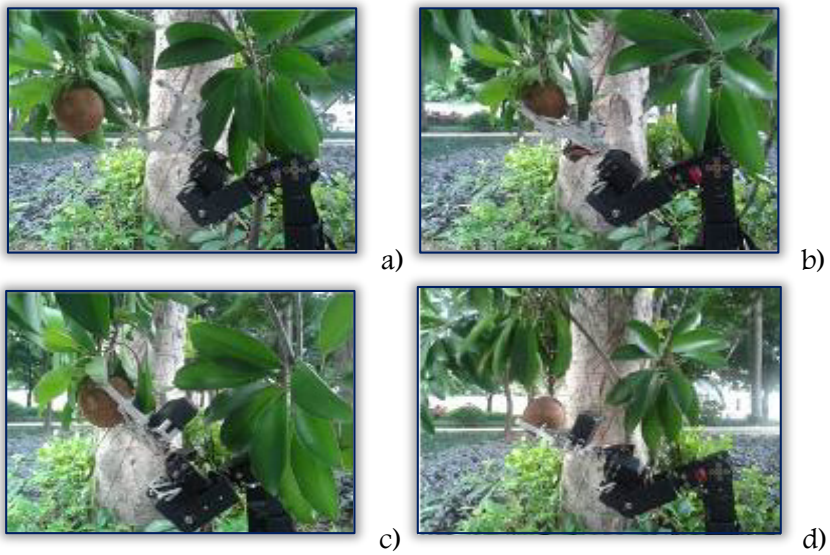

Figure 9 - Fruit picking process. (a) Start grabbing; (b) Finish grasping; (c) Start spinning; (d) Finish picking.

Table 6 shows how the PWM cycle affects the servo operation. When the PWM cycle is 2000 μs, the end-effector moves extremely fast, which is applicable for harvesting large fruits. When the cycle is 3000 μs, the speed is moderate, thus neither wearing off the machine because of the fast speed nor enabling harvesting because it is too slow. Therefore, the default PWM cycle utilized in this system is 3000 μs. Table 7 shows the test results of the precise movement of the end-effector to the target coordinates. This table shows that the end-effector is able to reach the space coordinates of the target transmitted by the binocular system, accurately analyze the direction of the coordinates, and determine the picking posture when harvesting. Moreover, picking robot can judge if the space coordinates are within the range of harvesting, which is in line with the system design. It means the end-effector can determine if the target can be picked; if not, the end-effector will have no movement and give the feedback to the PC end.

Table 6. PWM cycle and servo control

| PWM Cycle (us) | 1500 | 2000 | 3000 | 7000 |
|---|---|---|---|---|
| How the end-effector works | No movement | Extremely fast movement, normal operation | Moderately fast movement, normal operation | Slow movement, insufficient strength |

Table 7. Test results of the picking end-effector

| Space coordinates of the target (mm) | (150, 150, 156) | (100, 200, 156) | (100, 400, 256) | (–50, 100, 160) |
|---|---|---|---|---|
| Tested Results | Accurate picking | Accurate picking | Target can not be picked | Accurate picking |

## 6. CONCLUSIONS

The research on fruit picking robots is thriving in China and abroad because of its significance in the development of science and technology and human civilization. The picking end-effector is metal structure composed of five servos that control each junction of the end-effector to adapt complicated situations. The picking end-effector is more flexible and stable than other manipulators. In this paper, the movement in harvesting fruits is discussed; and each junction of the end-effector has mathematical modeling through which the coordinates of the target fruit is disassembled and analyzed so the end-effector can reach to the target precisely. Finally, experiments have verified the validity of the end-effector and its efficiency in agricultural operation.

**Acknowledgement:** This research was funded by the National Natural Science Foundation of China under Grant No.61505037, the National Spark Program under Grant No.2014GA780009, the State Scholarship Fund under Grant CSC No.201408440326,the Guangdong Natural Science Foundation under Grant No.S2013040014993, the Pearl River S&T Nova Program of Guangzhou under Grant No.201506010035, the University-sponsored Research Project of Guangdong University of Finance and Economics under Grant No.14GLL63001, the Research Project of Research Institute of Education

in Guangdong Province under Grant No.GDJY-2014-C-b043, the University Scientific Research Project of Guangxi Education Office under Grant No.KY2015ZL095.

## References

[1.] Berenstein Ron, ShaharOhad Ben, Shapiro Amir, Edan Yael. (2010) - Grape clusters and foliage detection algorithms for autonomous selective vineyard sprayer, Intelligent Service Robotics, vol. 3, no.4, pp. 233-243;
[2.] Blanes Carlos, Ortiz Coral, Mellado Martin, Beltrán Pablo. (2015) - Assessment of eggplant firmness with accelerometers on a pneumatic robot gripper, Computers and Electronics in Agriculture, vol. 113, pp. 44-50;
[3.] Chiu Yi-Chich, Yang P.Y., Chen S. (2013) - Development of the end-effector of a picking robot for greenhouse-grown tomatoes, Applied Engineering in Agriculture, vol. 29, no.6, pp. 1001-1009;
[4.] Chua P.Y., Ilschner T., Caldwell D.G., Van Henten E.J. (2003) - Robotic manipulation of food products - A review, Industrial Robot, vol. 30, no.4, pp. 345-354;
[5.] Edan Yael, Rogozin Dima, Flash Tamar, Miles Gaines E. (2000) - Robotic melon harvesting, IEEE Transactions on Robotics and Automation, vol. 16, no.6, pp. 831-835;
[6.] Elias Lopez-Alba, Ruben Dorado-Vicente, Jose Vasco-Olmo, Francisco Alberto Diaz-Garrido. (2012) - Design and development of a vibration clamp for agricultural purposes, vol. 87, no.1, pp. 114-119;
[7.] Hayashi S, Ganno K, Ishii Y, Tanaka K. (2002) - Robotic harvesting system for eggplants, Japan Agricultural Research Quarterly, vol. 36, no.3, pp. 163-168;
[8.] Hu Zhiyong, Zhang Xuewei, Zhang Wei, Wang Lin. (2014) - Precise control of clamping force for watermelon picking end-effector, Transactions of the Chinese Society of Agricultural Engineering, vol. 30, no.17, pp. 43-49;
[9.] Ji Chao, Feng Qingchun, Yuan Ting, Tan Yuzhi, Li Wei. (2011) - Development and performance analysis on cucumber harvesting robot system in greenhouse, Robot, vol. 33, no.6, pp. 726-730;
[10.] Jin Bo, Lin Longxian. (2014) - Design and force control of an underactuated robotic hand for fruit and vegetable picking, Journal of Mechanical Engineering, vol. 50, no.19, pp. 1-8;
[11.] Lin Hanhui, Cai Ken, Zeng Zhaofeng. (2015) - Design of a low-cost system with built-in-gps agricultural machinery, INMATEH - Agricultural Engineering, vol. 46, no.2, pp.25-36;
[12.] M. Mustafa Ertay, Ahmet Zengin. (2014) - Analysis of the discontinuous PWM controlled D-STATCOM for reactive power compensation applications, TehnickiVjesnik, vol. 21, no.4, pp. 825-833;
[13.] Reed J.N., Miles S.J., Butler J., Baldwin M., Noble R. (2001) - AE-automation and emerging technologies: automatic mushroom harvester development, Journal of Agricultural Engineering Research, vol. 78, no.1, pp. 15-23;
[14.] Shen Jian-Guang, Tao Tao, Mei Xue-Song, Xu Mu-Xun, Liu Shan-Hui. (2013) - An improved line-drawing algorithm for arbitrary fractional frequency divider/multiplier based on FPGA, Journal of Engineering Science and Technology Review, vol. 6, no.5, pp. 90-94;
[15.] Van Willigenburg L.G., Hol C.W.J., Van Henten E.J. (2004) - On-line near minimum-time path planning and control of an industrial robot for picking fruits, Computers and Electronics in Agriculture, vol. 44, no.3, pp. 223-237;
[16.] Wang Xuelin, Xiao Yongfei, Bi Shuhui, Fan Xinjian, Rao Honghui. (2015) - Design of test platform for robot flexible grasping and grasping force tracking impedance control, Transactions of the Chinese Society of Agricultural Engineering, vol. 31, no.1, pp. 58-63;
[17.] Xiong Juntao, Ye Min, ZouXiangjun, Peng Hongxing, Lin Guichao, Zhu Mengsi. (2013) - System design and performance analysis on multi-type fruit harvesting robot, Transactions of the Chinese Society for Agricultural Machinery, vol. 44, no.1, pp. 230-235;
[18.] Yan Lei, Yu Zheng, Han Ning, Liu Jinhao. (2013) - Improved image fusion algorithm for detecting obstacles in forests, Journal of Digital Information Management, vol. 11, no.5, pp. 378-384;
[19.] Ying Yibin, Zhang Wenying, Jiang Yiyuan, Zhao Yun. (2000) - Application of machine vision technique in automatic harvesting and processing of agricultural products,Transactions of the Chinese Society of Agricultural Machinery, vol. 31, no.3, pp. 112-115;
[20.] Yuan Ting, Xu Chen-Guang, Ren Yong-Xin, Feng Qing-Chun, Tan Yu-Zhi, Li Wei. (2009) - Detecting the information of cucumber in greenhouse for picking based on NIR image, Spectroscopy and Spectral Analysis, vol. 29, no.8, pp. 2054-2058;
[21.] Zhang Peng, Song Jian, Gong Shenglei, Jiang Bo, Muham Polar D. (2014) - A kinematic analysis and simulation based on ADAMS for eggplant picking robot, INMATEH - Agricultural Engineering, vol. 43, no.2, pp. 51-60;
[22.] Zhou Jun, Ji Changying. (2003) - Multi-resolution road recognition for vision navigation, Transactions of the Chinese Society for Agricultural Machinery, vol. 34, no.6, pp. 120-123.
[23.] Lin Hanhui, Cai Ken, Chen Huazhou, Zeng Zhaofeng, Optimization design of fruit pinking end-effector based on its grasping model, ISB-INMA TEH' 2015 International Symposium (Agricultural and Mechanical Engineering), 2015, pp. 499-508